

## Application and optimization of a quantified kinetic formula to mineral carbonation of natural silicate samples

Fei Wang<sup>a,\*</sup>, David Dreisinger<sup>a</sup>, Mark Jarvis<sup>b</sup>, Lyle Trytten<sup>b</sup>, Tony Hitchins<sup>b</sup>

<sup>a</sup> Department of Materials Engineering, The University of British Columbia, Vancouver, British Columbia V6T 1Z4, Canada

<sup>b</sup> Giga Metals Corporation, 203-700 West Pender Street, Vancouver, British Columbia V6C 1G8, Canada

### ARTICLE INFO

**Keywords:**

Mineral carbonation  
Natural silicate samples  
Quantified kinetic formula  
Olivine  
Chemical reaction control

### ABSTRACT

Mineral carbonation for global warming mitigation has attracted worldwide attention. The combination of mineral processing for primary metal recovery and mineral carbonation for carbon sequestration is an emerging field of study with the potential to minimize capital costs. A quantified kinetic formula of mineral carbonation was tested for application to various natural silicate samples. Our research confirms the optimized kinetic formula can be successfully applied to predict mineral carbonation of various natural silicate samples within absolute 4% precision. The kinetic factor is exponentially dependent on the activation energy of carbonation of natural silicate samples. The application of the kinetic formula is restricted to a mineral carbonation process under chemical reaction control. The successful application is not affected by mineral compositions, olivine content, mineral carbonation capacity, specific surface area, particle size distribution, temperature, CO<sub>2</sub> partial pressure or concentration of sodium bicarbonate in solution. This quantified kinetic formula can predict mineral carbonation efficiency for an integrated process of mineral processing and mineral carbonation.

### 1. Introduction

Mineral carbonation(Lackner, 2003; Sanna et al., 2014; Seifritz, 1990), both active(Pan et al., 2020; Renforth et al., 2011; Xi et al., 2016) and passive processes(Daval, 2018; Matter and Kelemen, 2009; Power et al., 2013; Tomkinson et al., 2013), has attracted worldwide attention owing to the formation of stable carbonate products(Daval, 2018; Matter et al., 2016; Matter and Kelemen, 2009; Pan et al., 2020; Renforth et al., 2011; Sanna et al., 2014; Tomkinson et al., 2013; Xi et al., 2016). However, the expensive capital cost of the mineral carbonation process limits its potential application(Olajire, 2013; Seifritz, 1990). To avoid the intensive energy consumption of materials pre-treatment for particle size reduction(Li and Hitch, 2016), it is suggested to combine active mineral carbonation with mineral processing(Wang et al., 2018) or other technologies(Bourgeois, 2019; Hamilton et al., 2020; International Energy Agency, 2016; Li et al., 2016). Mineral processing usually recovers targeted minerals by particle size reduction to liberate the target minerals. Many ultramafic mineral deposits contain various silicate minerals, including olivine(Béarat et al., 2006; Gadikota et al., 2014; Oelkers et al., 2018; Stopic et al., 2019; Wood et al., 2019), serpentine(Hamilton et al., 2020; Power et al., 2013) and pyroxene

(Hasan and Kusin, 2018; J. Wang et al., 2019c). The basic silicate minerals which are useful in mineral carbonation are generally considered as gangue minerals and discarded as finely-ground waste tailings(Hitch and Dipple, 2012). The previous research studies have shown that there were different mineral carbonation behaviours between olivine and other minerals(O'Connor et al., 2005, 2001; Wang et al., 2021). Carbonation of olivine was usually the dominant chemical reaction of a direct aqueous mineral carbonation process under intermediate CO<sub>2</sub> partial pressure conditions<sup>8</sup>. Unless serpentine is heat pre-treated, the carbonation rate is significantly slower than the reaction of olivine(O'Connor et al., 2005, 2001; Wang et al., 2021).

Our previous studies(F. Wang et al., 2019b) have developed a quantified kinetic formula from mineral carbonation of a high-grade olivine, as shown in Equation (1).

$$\alpha = \left( 1 - \left( 1 - k^o \times [S]^{0.7} \times [P_{CO_2}]^{1.6} \times [NaHCO_3]^{0.8} \times e^{(-Ea \times 1000/RT)} \times t \right)^3 \right) \times 100\% \quad (1)$$

where  $\alpha$  is mineral carbonation efficiency, %; [S] is the specific surface area of the material, m<sup>2</sup>/g; [PCO<sub>2</sub>] represents CO<sub>2</sub> partial

\* Corresponding author.

E-mail address: fei.wang@alumni.ubc.ca (F. Wang).

**Table 1**

Quantified mineral compositions and lithologies of various natural silicate samples.

Minerals \ Lithology	Natural silicate samples								
	Dunite					Serpentinized wehrlite			Wehrlite
	SN254	SN255	SN256	SN257	SN258	SN259	SN260	SN261	SN262
Olivine (Mg, Fe) <sub>2</sub> SiO <sub>4</sub>	83.5	78.7	80.4	85.0	79.5	50.5	40.1	30.2	73.3
Brucite Mg(OH) <sub>2</sub>	2.0	2.9	1.3	0.8	-	-	-	-	0.3
Quartz SiO <sub>2</sub>	0.4	0.3	0.3	0.3	-	0.4	-	-	-
Magnetite Fe <sub>3</sub> O <sub>4</sub>	3.8	5.5	5.9	3.9	3.9	6.4	4.4	10.0	4.6
Troilite FeS	-	-	0.5	1.7	4.6	0.5	8.1	1.3	2.0
Pyrrhotite Fe <sub>1-x</sub> S	-	-	-	-	-	1.3	11.4	1.7	2.8
Calcite CaCO <sub>3</sub>	-	-	0.5	0.4	0.3	0.3	2.5	1.1	0.7
Diopside CaMgSi <sub>2</sub> O <sub>6</sub>	-	-	-	-	4.9	29.4	4.9	12.5	9.1
Serpentine Mg <sub>3</sub> Si <sub>2</sub> O <sub>5</sub> (OH) <sub>4</sub>	9.5	12.6	11.2	8.0	6.8	11.1	28.6	43.3	7.2
Others	0.8	-	-	-	-	-	-	-	-
Total	100.0	100.0	100.0	100.0	100.0	100.0	100.0	100.0	100.0

pressure in the range of 28–41 bar; [NaHCO<sub>3</sub>] is the concentration of sodium bicarbonate in the range of 0.5–1.5 molality; Ea is the activation energy of mineral carbonation of high-grade olivine, 47.97 kJ/mol; R is the Gas Constant, 8.314 J·mol<sup>-1</sup>·K<sup>-1</sup>; T is reaction temperature in the range of 273–448 K; and t is reaction time, hour. k° is a kinetic factor, also called as correction factor on our previous research (F. Wang et al., 2019b).

This formula developed from a high-grade olivine can potentially predict the mineral carbonation efficiency and the process conditions required to carry out a carbonation process. However, application to natural silicate mixtures is more realistic and may encounter challenges. The different mineral carbonation behaviour of different minerals may affect the application of this quantified kinetic formula. Furthermore, factors affecting the kinetic factor k° are not well understood. This research was designed to test the application of this formula to the mineral carbonation of various natural silicate samples in partially-serpentinitized ultramafic deposit and to optimize this kinetic formula for robust application.

## 2. Materials and methodology

### 2.1. Materials

The natural silicate samples were obtained from the Turnagain

nickel–cobalt and partially serpentinitized ultramafic deposit located in northern British Columbia of Canada, and were provided by Giga Metals Corporation. The nine silicate samples belong to a variety of lithologies including dunite, wehrlite, and serpentinitized wehrlite, as shown in Table 1. The corresponding mineral compositions are shown in Table 1. These samples have a range of mineral compositions, especially with respect to the content of olivine, diopside and serpentine. The dunite samples SN254-SN258, have the highest olivine content (80%–85%) and the lowest contents of diopside and serpentine (total 8%–13%). The wehrlite sample SN262 has 73% olivine and a total of 18% diopside and serpentine. In contrast, the serpentinitized wehrlite samples SN259-SN261 have much lower olivine content, ranging from 50% to 30%. Sample SN259 has the highest diopside content of 29% together with 11% serpentine; Sample SN260 has the highest content of iron sulfides (including troilite and pyrrhotite) at 20% together with 29% serpentine; Sample SN261 has the lowest (30%) olivine and the highest (43%) serpentine together with 13% diopside. The diopside, serpentine and iron sulfides are not expected to be involved in the mineral carbonation process based on previous research (Wang et al., 2021).

The chemical compositions of these natural samples are shown in Table 2. The original carbon content for all samples is very low, <0.1%. The sulfur content varies up to 7% with the iron sulfide content of samples. There are also valuable metals including nickel, cobalt and copper, which are targets for recovery via mineral processing. The major

**Table 2**

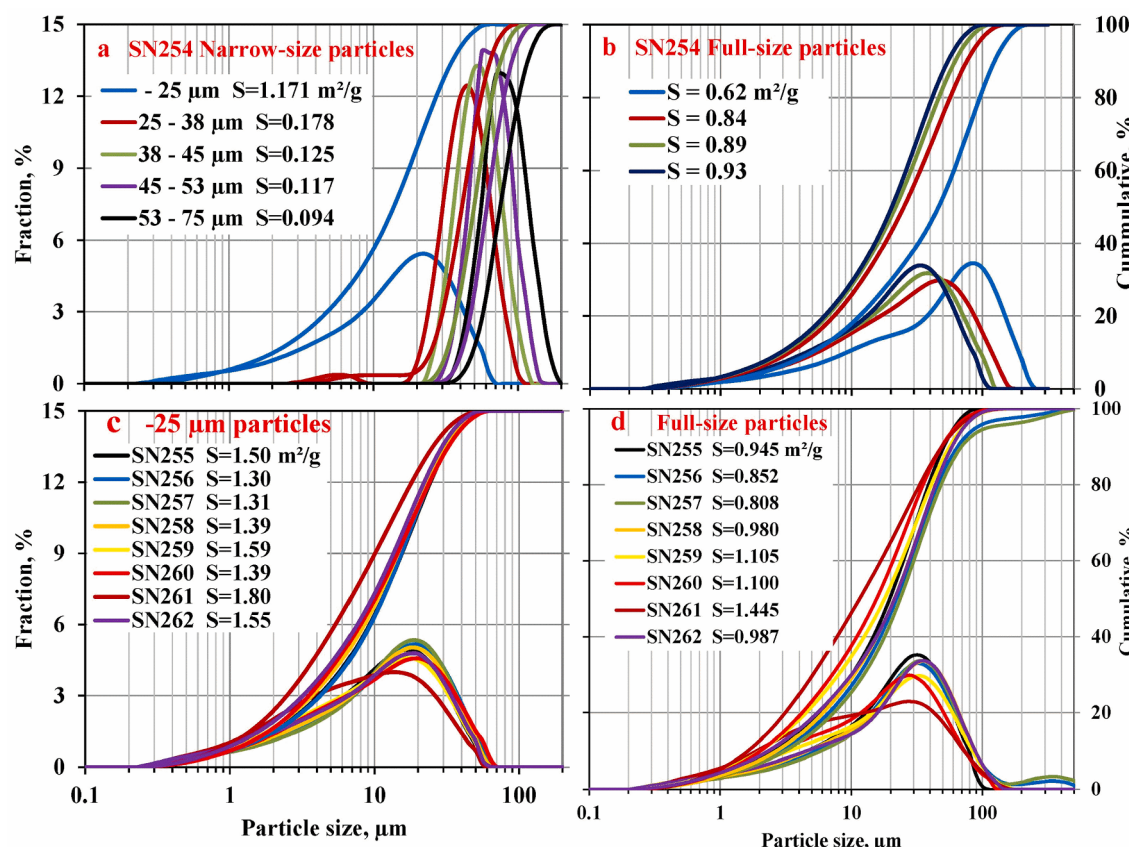
Chemical compositions of Turnagain samples.

Samples	SN254	SN255	SN256	SN257	SN258	SN259	SN260	SN261	SN262
S, %	0.03	0.04	0.83	1.30	2.16	1.13	7.19	1.40	2.30
Ni, %	0.28	0.26	0.32	0.35	0.26	0.23	0.70	0.33	0.40
Mg, %	24.14	23.83	22.85	22.74	22.47	18.32	18.24	19.07	21.21
Fe, %	6.60	6.45	8.01	8.99	10.06	7.88	15.62	7.79	9.77
Co, %	0.01	0.01	0.02	0.02	0.02	0.01	0.05	0.02	0.02
Cu, %	<0.01	<0.01	0.04	0.07	0.03	0.03	0.20	0.05	0.09
Al, %	0.04	0.05	0.13	0.04	0.06	0.58	0.22	0.44	0.19
Ca, %	0.21	0.15	0.29	0.24	0.57	3.90	0.51	1.21	1.05
K, %	<0.01	<0.01	0.03	<0.01	<0.01	0.12	0.03	0.09	0.02
Na, %	<0.01	<0.01	<0.01	<0.01	<0.01	0.03	<0.01	<0.01	0.01
C, %	0.06	0.11	0.10	0.05	0.06	0.05	0.03	0.05	0.04

**Table 3**

Mineral carbonation capacity of Turnagain samples SN254 – SN262.

Mineral carbonation capacity, t CO <sub>2</sub> /t	SN254	SN255	SN256	SN257	SN258	SN259	SN260	SN261	SN262
m <sub>o</sub> <sup>a</sup>	0.49	0.48	0.48	0.49	0.49	0.44	0.46	0.42	0.47
m <sub>o'</sub> <sup>b</sup>	0.47	0.38	0.38	0.41	0.39	0.22	0.17	0.12	0.34

<sup>a</sup> : m<sub>o</sub> is based on the contents of total magnesium, total iron and total calcium.<sup>b</sup> : m<sub>o'</sub> is based on the contents of magnesium and iron only in olivine.**Fig. 1.** Particle size distributions of various natural silicate samples: a) narrow-size particles of sample SN254; b) full-size particles of sample SN254; c) –25 μm particles of samples SN255-SN262; and d) full-size particles of samples SN255-SN262.

targets of mineral carbonation are the minerals containing the elements of magnesium, iron and calcium. These elements can, in principle, form stable metal carbonates. Magnesium is mainly in the form of olivine and the other silicates with the content varying from approximately 18% for serpentinized wehrlite samples to about 23% for dunite samples. Calcium is mainly in the mineral of diopside. The calcium content is 3.9% for sample SN259 and <1% for others. The occurrence of iron is more complicated. Iron is in the form of magnetite and iron sulfides in addition to olivine and the other silicates by substituting for magnesium in the crystal structure. The content of iron for all samples is in the range of 6.5%-10%, except for sample SN260 with 16% iron due to the high content of iron sulfides. The contents of sodium and potassium are not considered for permanent carbon storage in this research as the carbonates of these elements are highly soluble. The mineral carbonation capacity m<sub>o</sub> for each sample is calculated based on the content of total magnesium, iron and calcium as shown in Equation (2).

Previous research (Wang et al., 2021) has confirmed that the dominant chemical reaction during mineral carbonation of natural silicate samples is the carbonation of olivine. The corresponding mineral carbonation process is controlled by the dissolution of olivine. Magnetite, iron sulfides (troilite and pyrrhotite) and diopside did not react. The kinetic analysis should be carried out according to the transformed

mineral carbonation capacity m<sub>o'</sub>, which is based on the contents of magnesium and iron in olivine as shown in Equation (3). The comparison of the original and transformed mineral capacity is shown in Table 3.

$$m_o = \left( \frac{[Mg]}{24.305} + \frac{[Fe]}{55.845} + \frac{[Ca]}{40.078} \right) \times 44.01 \quad (2)$$

$$m_{o'} = m_o - m_{o''} \quad (3)$$

where, m<sub>o</sub> is the mineral carbonation capacity based on the contents of total magnesium, iron and calcium; m<sub>o'</sub> is the mineral carbonation capacity based on the contents of magnesium and iron in olivine; m<sub>o''</sub> is the mineral carbonation capacity based on the contents of iron in magnetite and iron sulfides (troilite and pyrrhotite) and the contents of magnesium and calcium in diopside, t CO<sub>2</sub>/t sample.

## 2.2. Methods

All the silicate samples were ground in a rod mill under the conditions of 60% solids and 1 kg sample/16.5 kg rod charge followed by wet-screening to obtain the narrow-sized particle fractions. The sieves sizes 500 mesh, 400 mesh, 325 mesh, 270 mesh and 200 mesh were used for

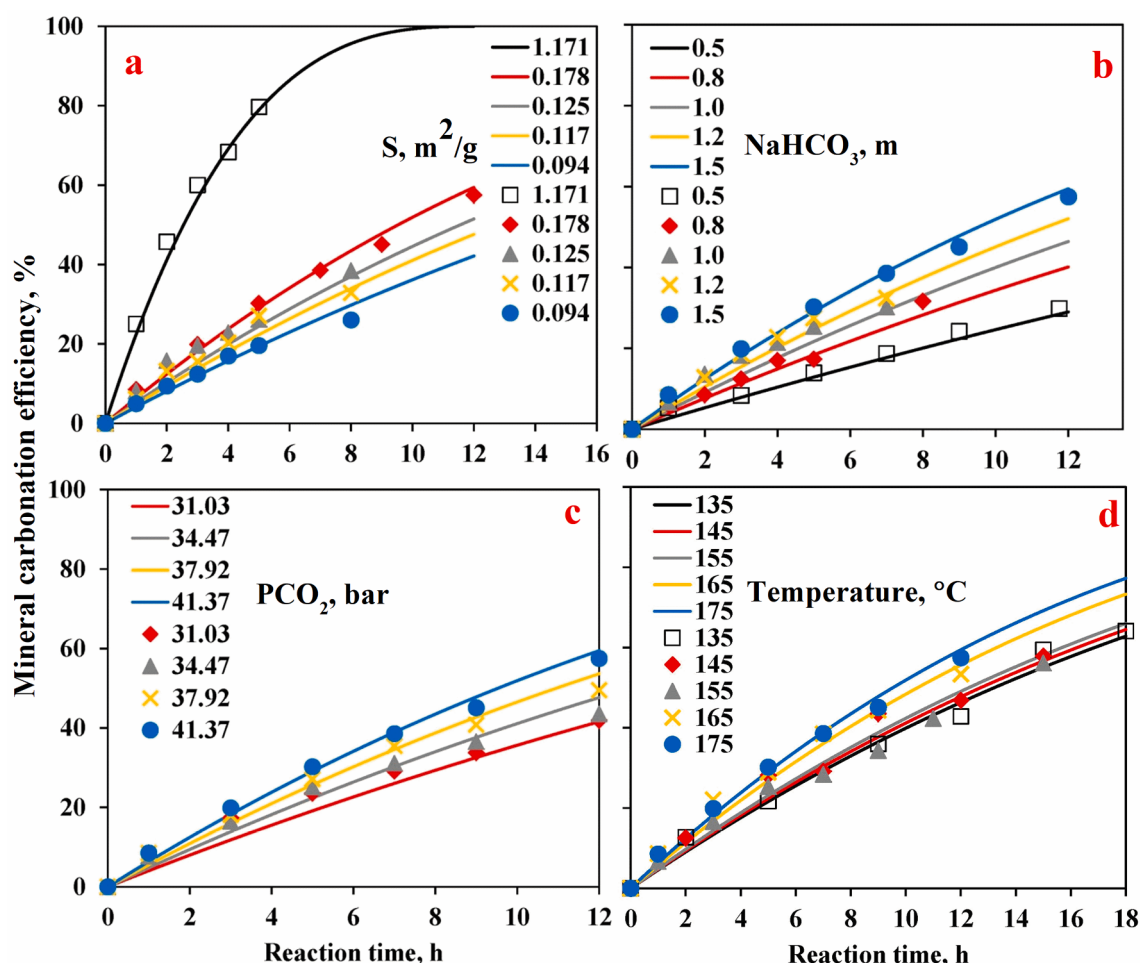


**Fig. 2.** Comparison of the experimental data and the predicted data from the quantified kinetic formula under the conditions of 25–38 µm particle size fractions,  $\text{PCO}_2 = 41.4 \text{ bar}$ , 175 °C, 10% solids content with 1.5 M NaHCO<sub>3</sub>; (a) for effects of specific surface area; (b) for effects of addition of NaHCO<sub>3</sub>; (c) for effects of  $\text{PCO}_2$ ; (d) for effects of temperature and  $k^\circ = 135, 100, 75, 65$  and 53 at 135 °C, 145 °C, 155 °C, 165 °C and 175 °C, respectively, for dunite sample SN254.

the wet-screening to acquire the narrow-sized particle fractions, – 25 µm, 25–38 µm, 38–45 µm, 45–53 µm and 53–75 µm. The full size-range particles were the products of grinding without screening. The corresponding particle size distributions and specific surface areas of all the narrow- and full-size particles were determined by the Malvern Mastersizer 2000, as shown in Fig. 1.

The carbonation tests were carried out in a 600 mL high temperature reactor (Parr instrument, model 5103). Prior to the tests, the samples were loaded into the reactor vessel with 400 mL of aqueous solution which contained sodium bicarbonate. The slurry was mixed at room temperature with 300 rpm agitation speed. High-purity CO<sub>2</sub> gas was introduced into the vessel to a total pressure of 6.9 bar and then released to 0.1 bar pressure followed by increasing the total pressure to 1.4 bar. This method was used first to remove most of the air from the autoclave and second to seal the reactor, respectively. The reactor was then heated to the pre-determined temperature within approximately 20 min. Once the desired temperature was reached, the reaction time started to be recorded. The agitation speed was increased up to 700 rpm and high-purity CO<sub>2</sub> gas was introduced to the pre-determined target pressure in approximately one minute, where the CO<sub>2</sub> partial pressure was the difference between the total pressure and the water vapour pressure calculated at that temperature. When the test was complete, the reactor was cooled down to room temperature and the pressure was released starting from the temperature at around 50 °C. After the test, the cooled slurry was filtered with vacuum. The solids were washed five times by deionized water, followed by drying to remove free moisture in an oven

at 60 °C for 12 h, and analysis for total carbon content.

The nine natural silicate samples were analyzed by Inductively Coupled Plasma – Optical Emission Spectrophotometry (ICP-OES) analysis after lithium borate fusion for most elements, and after four-acid (hydrochloric acid, nitric acid, hydrofluoric acid and perchloric acid) digestion for copper and cobalt. The total carbon and sulfur content were analyzed by the LECO CS3200 instrument. The carbon contents before and after reaction were used for the calculation of mineral carbonation efficiency. The mineral composition analysis was via the Quantitative X-ray Diffraction (QXRD) method with Rietveld refinement. The amounts of serpentine were analyzed based on the PONKCS method(Falini et al., 2004; Scarlett and Madsen, 2006) for samples SN260-SN261 and the Rietveld refinement using the lizardite-1 T crystal structure(Mbrtrnr, 1982) for all the other samples with  $R_{wp}$  (weighted profile R-factor) values<6.0. All the  $R_{wp}$  values for the QXRD analysis are<6.0.

The evaluation of mineral carbonation efficiency ( $\alpha$ ) derives from considering the final fate of CO<sub>2</sub> gas during the mineral carbonation above 100 °C, which is formation of non-hydrous carbonates. The corresponding calculation formula is shown in Equation (4) (F. Wang et al., 2019a, 2019b), which is only based on the carbon contents before and after mineral carbonation and the theoretically maximum carbonation capacity. The amount of sequestered CO<sub>2</sub> gas ( $m_{\text{CO}_2}$ ) for each tonne raw material is based on the mineral carbonation efficiency and the maximum carbonation capacity, as shown in Equation (5).

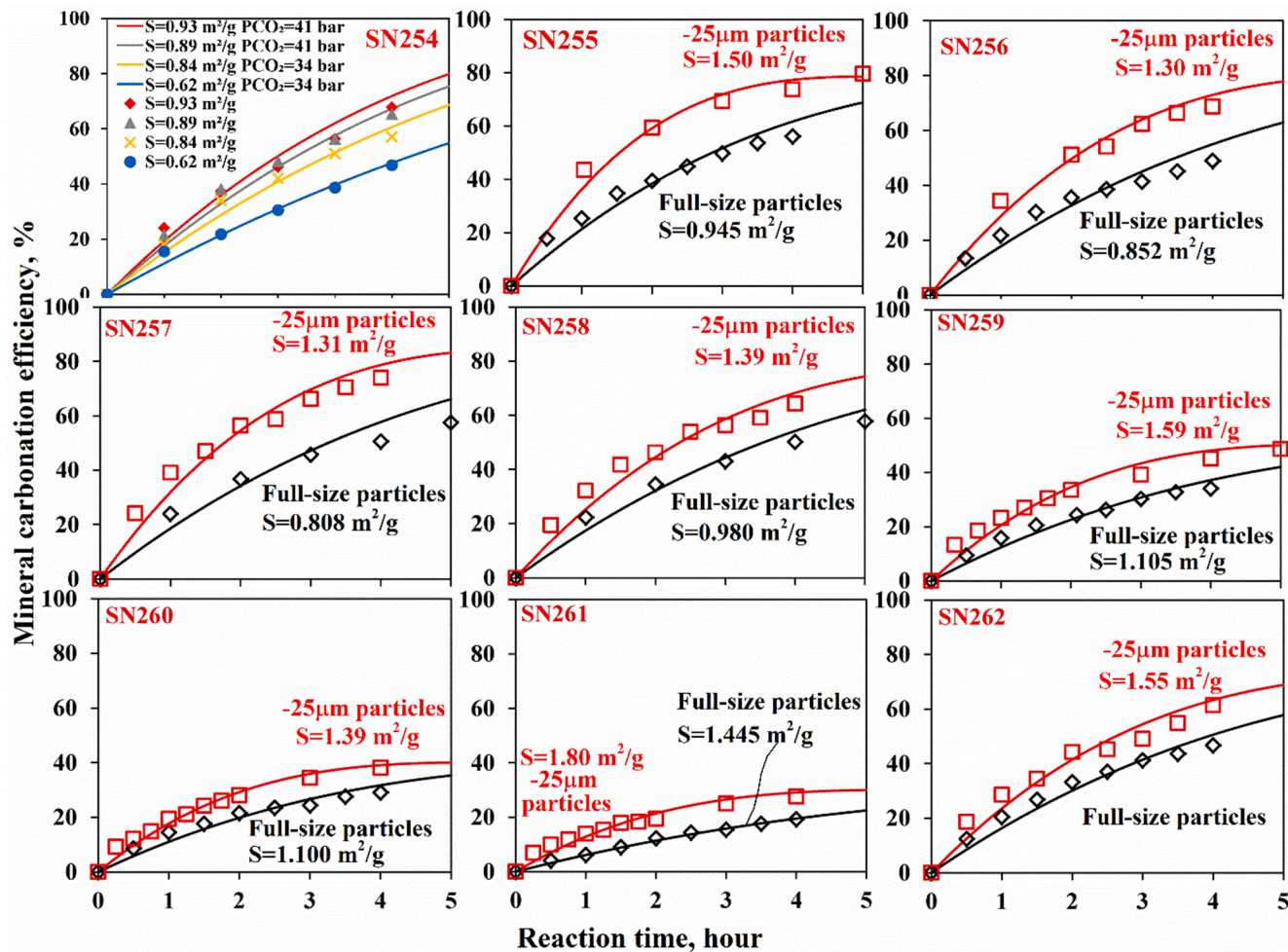


**Fig. 3.** Application of the quantified kinetic formula to mineral carbonation of various natural silicate samples under the conditions of 175 °C, PCO<sub>2</sub> = 34.5 bar, 1.5 m NaHCO<sub>3</sub> and 10% pulp density.

$$\alpha = \frac{\theta_2 - \theta_1}{m_o \times (\frac{12.011}{44.098} - \theta_2)} \quad (4)$$

$$m_{CO_2} = \alpha \times m_o \quad (5)$$

where,  $\theta_1$  and  $\theta_2$  are the total carbon content in %, of the solid before and after carbonation, respectively; and  $\alpha$  is the mineral carbonation efficiency in %;  $m_o$  is the maximum mineral carbonation capacity of the raw materials with unit of t CO<sub>2</sub>/t material as shown in Table 3; and  $m_{CO_2}$  is the amount of sequestered CO<sub>2</sub> gas, with unit of t CO<sub>2</sub>/t material.

### 3. Results and discussions

#### 3.1. Application to a natural dunite sample

The natural silicate sample SN254 is the least complex sample among all the Turnagain samples, dominantly olivine and serpentine and lacking sulfides. The first application is to narrow-sized particle fractions of sample SN254: – 25 μm; 25 – 38 μm; 38 – 45 μm; 45 – 53 μm; and 53 – 75 μm, as shown in Fig. 1(a). The corresponding calculated specific surface areas are 1.171, 0.178, 0.125, 0.117 and 0.094 m<sup>2</sup>/g, respectively. The mineral carbonation tests were mainly performed under the condition of 25 – 38 μm particle size, CO<sub>2</sub> partial pressure PCO<sub>2</sub> = 41 bar, 175 °C, 10% solids content with 1.5 m NaHCO<sub>3</sub>. The results and the comparison with the prediction based on the kinetic formula are shown in Fig. 2.

As illustrated in Fig. 2(a), all the experimental results for all the

particle size fractions and the predicted data matched well for the reaction times of 12 h, 8 h or 5 h. It is also noted that the kinetic factor  $k^\circ$  value needed to be adjusted to 53 for Turnagain sample SN254. The application of the quantified kinetic formula under the effect of sodium bicarbonate concentration is shown in Fig. 2(b). In order to demonstrate that the carbonation rate was controlled by chemical reaction, the range of the sodium bicarbonate concentration was from 0.5 m to 1.5 m (F. Wang et al., 2019a). It is obvious that the agreement between experimental results and the kinetic formula prediction was excellent for this Turnagain sample SN254. Similar close matches between the experimental and predicted data were also observed for varying CO<sub>2</sub> partial pressure (Fig. 2(c)). The PCO<sub>2</sub> ranged from 31 bar to 41 bar so that the mineral carbonation process was controlled by the dissolution of olivine rather than by diffusion through a carbonate product layer (F. Wang et al., 2019a). The temperature effect was tested with PCO<sub>2</sub> = 41 bar and with 1.5 m NaHCO<sub>3</sub>, where the carbonation process was still controlled by chemical reaction. Unfortunately, in order to achieve the good match between the experimental and predicted data from the direct kinetic formula application, the kinetic factor  $k^\circ$  varied with temperature as shown in Fig. 2(d). The suitable  $k^\circ$  at 135 °C, 145 °C, 155 °C, 165 °C and 175 °C were 135, 100, 75, 65 and 53, respectively. This wide variation of kinetic factor with temperature is a significant concern for potentially direct application of the kinetic formula. As the preceding research demonstrates, temperature, PCO<sub>2</sub>, particle size and sodium bicarbonate are the most important factors affecting the mineral carbonation process (F. Wang et al., 2019a). Thus far, data illustrated in Fig. 2 confirms that the quantified formula can be potentially applied in the carbonation of

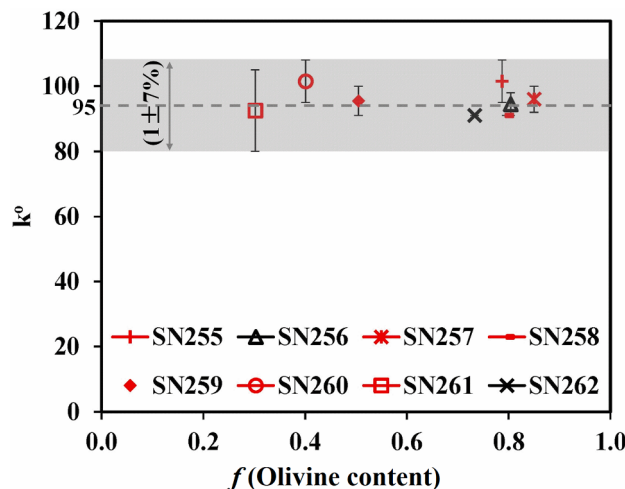


Fig. 4. Relationship between  $k^\circ$  and olivine content of Turnagain samples SN255-262.

narrow-sized sample SN254 at a temperature, although the varying kinetic factor  $k^\circ$  with temperature is a concern needing to be optimized.

In practical application of a metal recovery process, the requirement for particle size distribution usually is characterized by the  $P_{80}$ , such as  $P_{80} = 75 \mu\text{m}$  or  $P_{80} = 90 \mu\text{m}$ . Herein, the full-size range particles were further tested for matching of the formula to experiments under the conditions of  $\text{PCO}_2 = 41.4 \text{ bar}$  or  $34.5 \text{ bar}$ ,  $175^\circ\text{C}$ , 10% solids content with  $1.5 \text{ M NaHCO}_3$ , as shown in Fig. 3(a). The particle size distribution for the full-sized particles is shown in Fig. 1(b). The  $P_{80}$  for the four sets of samples was  $41 \mu\text{m}$ ,  $46 \mu\text{m}$ ,  $56 \mu\text{m}$  and  $93 \mu\text{m}$  with the corresponding specific surface area of  $0.93$ ,  $0.89$ ,  $0.84$  and  $0.62 \text{ m}^2/\text{g}$ , respectively. Again, the kinetic formula prediction fit well to the experimental data as shown in Fig. 3(a). As a result, the application of the quantified kinetic formula to the carbonation of dunite sample SN254 was successful under various conditions except for varying temperatures.

### 3.2. Application to various natural silicate samples

Previous research (Wang et al., 2021) has revealed that the carbonation of olivine is the dominant reaction during mineral carbonation of a natural mixture of minerals. The mineral carbonation of olivine is always controlled by chemical reaction of olivine dissolution once the sodium bicarbonate concentration is more than 0.5 molality and  $\text{PCO}_2$  is more than 28 bar (Wang et al., 2019a). The quantified kinetic formula, therefore, is potentially applicable to all the natural silicate samples. As shown in Fig. 3, the predicted data from the kinetic formula had a sufficiently good match with all the experimental data for all the natural silicate samples ground to  $-25 \mu\text{m}$  particles (particle size distribution shown in Fig. 1(c)) and a full-range size particles (particle size distribution shown in Fig. 1(d)). The maximum difference between the experimental data and the predicted data for all the conditions was at most 8% (absolute). Though the mineral carbonation efficiency for Turnagain SN261 was only around 20%, the kinetic formula prediction still matched the experimental data well. It is noted that the mineral carbonation efficiency calculated by the kinetic formula, Equation (1), is discounted in proportion to the olivine content ( $f$ ) of the natural silicate samples for the successful match. Therefore, Equation (1) is correspondingly optimized into Equation (6).

$$\alpha = \left( 1 - \left( 1 - k^\circ \times [S]^{0.7} \times [P_{\text{CO}_2}]^{1.6} \times [\text{NaHCO}_3]^{0.8} \times e^{(-E_a \times 1000/RT)} \times t \right)^3 \right) \times f \quad (6)$$

where,  $f$  is olivine content of natural silicate samples as shown in

Table 1.

In addition, when the activation energy was considered as a constant for direct application of the kinetic formula to mineral carbonation of olivine in natural samples, the most suitable kinetic factor  $k^\circ$  values for all the Turnagain samples SN255-SN262 are shown in Fig. 4. The kinetic factor  $k^\circ$  value for each sample is in the range of  $95(1 \pm 7\%)$ . Unfortunately, there is no specific relationship between the kinetic factor and the olivine content of each sample. It is still needed to manually adjust the  $k^\circ$  value and thus the kinetic formula is still semi-empirical thus far. In order to discover any general law among all the natural silicate samples, it is necessary to continue the following discussions on the value of  $k^\circ$ .

### 3.3. Optimization of the kinetic formula

According to the preceding discussions, the application of the kinetic formula had significant concerns on the determination of kinetic factor  $k^\circ$ , especially at varying temperatures. This kinetic formula needed to be further optimized for robust application. In order to determine the general law of the kinetic value  $k^\circ$  for all natural silicate samples, activation energy for Turnagain samples SN255 and SN258-262 was studied, as shown in Fig. 5. Our previous research (Wang et al., 2021) has shown that  $m_0'$  mineral carbonation capacity based on the contents of magnesium and iron in olivine (which is shown in Table 3) should be used for kinetic analysis; the mineral carbonation process should be controlled by surface chemical reaction of olivine dissolution, as shown in linear relationship between  $1 - (1 - \alpha)^{1/3}$  and reaction time  $t$ . Correspondingly, the mineral carbonation efficiency based on  $m_0'$  under temperatures from  $145^\circ\text{C}$  to  $175^\circ\text{C}$  is shown Fig. 5(a) for kinetic analysis. The fitting of  $1 - (1 - \alpha)^{1/3}$  versus  $t$  is also linear with  $R^2 \geq 0.94$ , as shown in Fig. 5(b).

The activation energy for each sample is shown in Fig. 5(c). It is in the range of  $14 - 25 \text{ kJ/mol}$ . It is not  $47.97 \text{ kJ/mol}$  in the original kinetic formula anymore because only olivine which was associated with other unreactive minerals in the natural silicate samples participated in the mineral carbonation reaction. Once the activation energy was optimized in the kinetic formula for each natural sample, the suitable kinetic factor  $k^\circ$  was correspondingly optimized as shown in Table 4. Similarly, the activation energy for dunite SN254 and SN256 can be also calculated as  $10.46 \text{ kJ/mol}$  and  $14.81 \text{ kJ/mol}$ , respectively. The corresponding  $k^\circ$  was  $0.0021$  and  $0.016$  for SN254 and SN256, respectively. As a result, Table 4 lists the detailed kinetic data for the high-grade olivine and various natural silicate samples with kinetic factor from direct application of the original kinetic formula and the optimized formula. It can be found that the kinetic constant,  $k_2$ , for chemical reaction control model was generally bigger for carbonation of natural silicate samples than carbonation of the high-grade olivine. It means that the natural silicate samples may be easier to sequester  $\text{CO}_2$  via mineral carbonation than the high-grade olivine. Furthermore, the relationship between  $k^\circ$  and activation energy for each Turnagain sample is shown in Fig. 6. The  $k^\circ$  is exponentially determined by activation energy of mineral carbonation with  $R^2$  greater than 0.98 for both high-grade olivine and Turnagain samples. This relationship can be shown in Equation (7), where  $E_a$  is activation energy for each sample;  $A = 30.74 \text{ kJ/mol}$  and  $B = 3.70$  and the accuracy of  $A$  and  $B$  can be improved with more experimental data from more natural silicate samples added to Fig. 6.

$$k^\circ = e^{\frac{E_a - A}{B}} \quad (7)$$

On the other hand, there is no clear relationship between olivine content and activation energy, as shown in Fig. 7. It means that although the carbonation of olivine is the dominant reaction during mineral carbonation of natural silicate samples, the activation energy is comprehensively determined by various factors of natural samples including olivine content, mineral composition and also the complicated behaviour of silica in high-temperature aqueous solution.

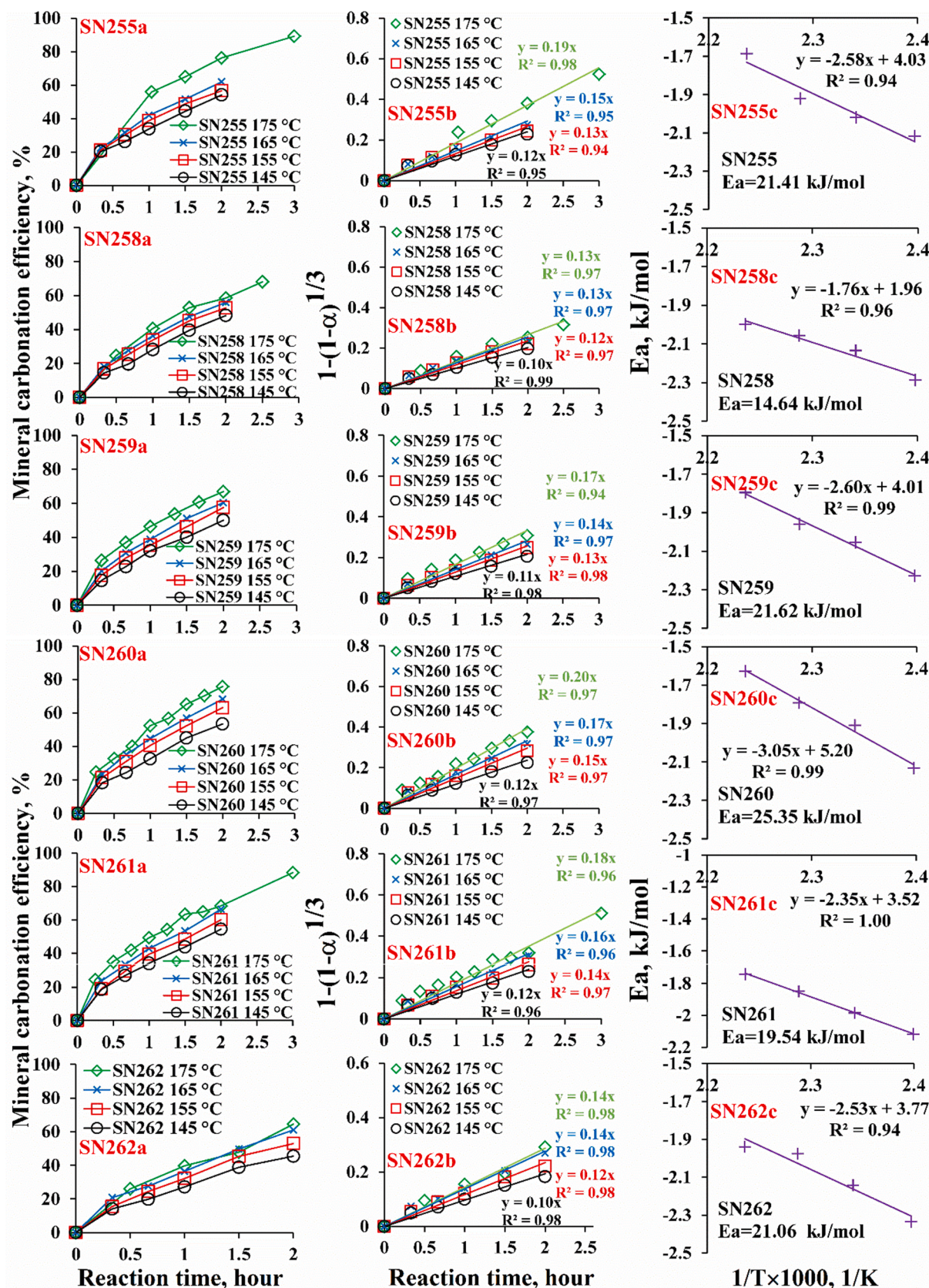


**Fig. 5.** Kinetic analysis of Turnagain samples SN255, SN258-262 under the conditions of  $\text{PCO}_2 = 34.5$  bar, 1.5 m  $\text{NaHCO}_3$  and 10% pulp density: a) Mineral carbonation efficiency based on magnesium and iron contents in olivine; b)  $1-(1-\alpha)^{1/3}$  vs t and c) Activation energy.

**Table 4**Kinetics for natural silicate samples on  $\text{PCO}_2 = 34.5$  bar and 1.5 M  $\text{NaHCO}_3$ .

Silicate sample	Specific surface area, $\text{m}^2/\text{g}$	Temperature °C	$k_2$	Ea kJ/mol	$k^\circ$	Note
High-grade Olivine	1.53	175	0.071	47.97	72	The original kinetic formula was derived from here
		175 (1 M $\text{NaHCO}_3$ )	0.067			
		165 (1 M $\text{NaHCO}_3$ )	0.059			
		155 (1 M $\text{NaHCO}_3$ )	0.032			
		135 (1 M $\text{NaHCO}_3$ )	0.021			
		120 (1 M $\text{NaHCO}_3$ )	0.012			
Turnagain samples	SN254	175 ( $\text{P}_{\text{CO}_2} = 41$ bar)	0.090	10.46	0.0021	$k^\circ=53$ direct application
		175 ( $\text{P}_{\text{CO}_2} = 41$ bar)	0.022			$k^\circ=53$
		165 ( $\text{P}_{\text{CO}_2} = 41$ bar)	0.021			$k^\circ=65$
		155 ( $\text{P}_{\text{CO}_2} = 41$ bar)	0.020			$k^\circ=75$
		145 ( $\text{P}_{\text{CO}_2} = 41$ bar)	0.018			$k^\circ=100$
		135 ( $\text{P}_{\text{CO}_2} = 41$ bar)	0.017			$k^\circ=135$
	SN255	175	0.19	21.41	0.098	$k^\circ=80$ (direct application)
		165	0.15			
		155	0.13			
		145	0.12			
SN256	1.30	175	0.20	14.81	0.016	$k^\circ=76$ for 175 °C (direct application)
		165	0.19			
		155	0.17			
		145	0.15			
SN257	1.31	175	0.14	–	82 (direct application)	
SN258	1.39	175	0.136	14.64	0.014	$k^\circ=72$ for 175 °C (direct application)
		165	0.127			
		155	0.118			
SN259	1.59	175	0.17	21.62	0.104	$k^\circ=48$ for 175 °C (direct application)
		165	0.14			
		155	0.13			
		145	0.11			
SN260	1.39	175	0.20	25.35	0.33	$k^\circ=41$ for 175 °C (direct application)
		165	0.17			
		155	0.15			
		145	0.12			
SN261	1.80	175	0.18	19.54	0.052	$k^\circ=28$ for 175 °C (direct application)
		165	0.16			
		155	0.14			
		145	0.12			
SN262	1.55	175	0.144	21.06	0.101	$k^\circ=67$ for 175 °C (direct application)

Therefore, the kinetic factor  $k^\circ$  is determined by activation energy of carbonation for each natural silicate sample. With comprehensive consideration of Equation (6) and (7), the kinetic formula can be optimized into Equation (8).

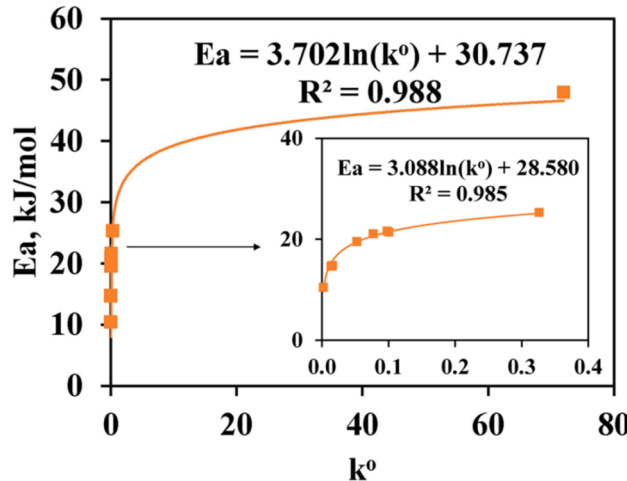
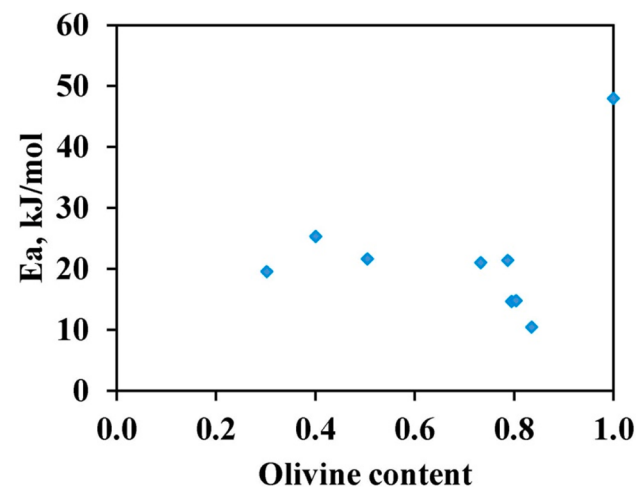
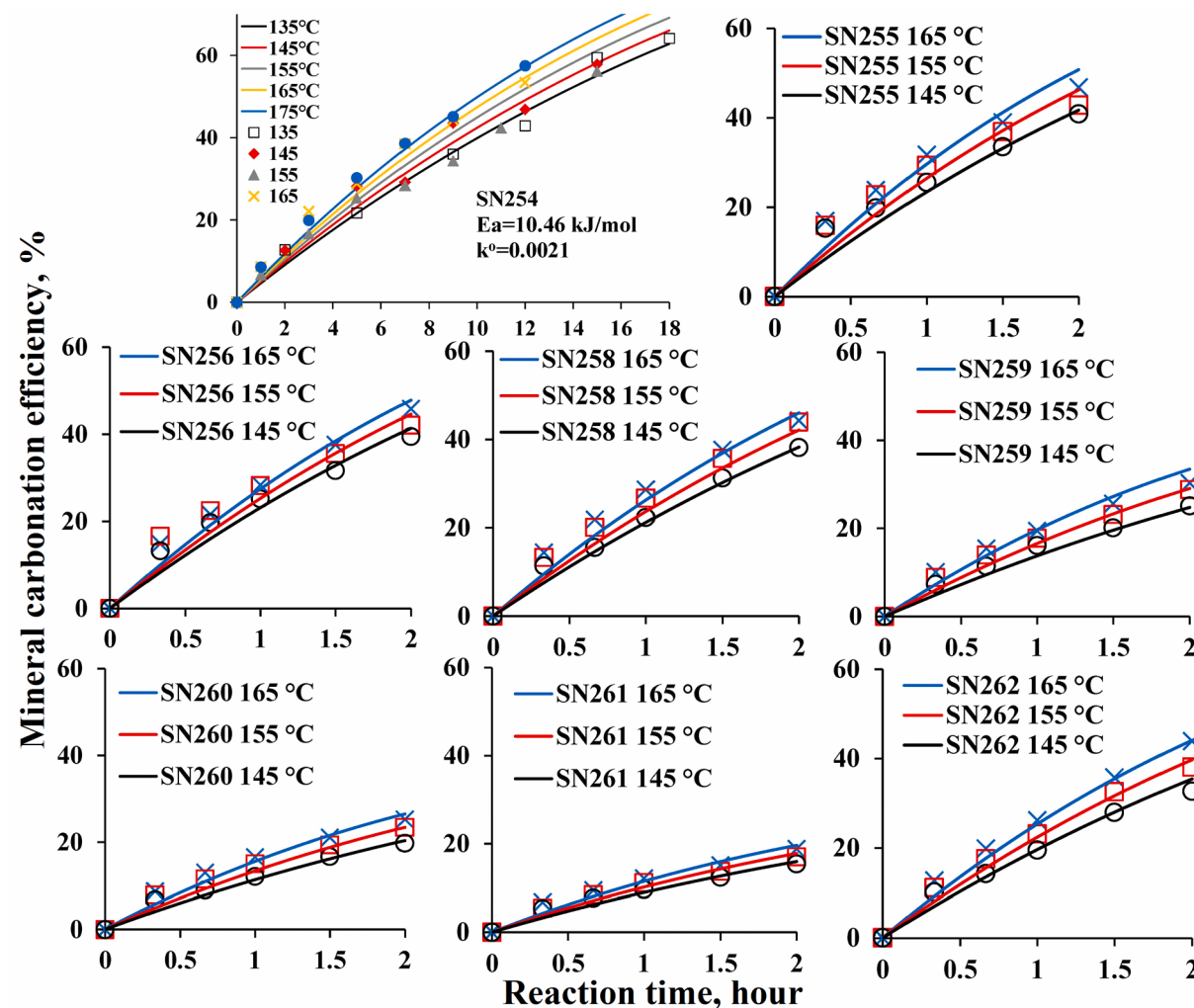
Fig. 6. Relationship between activation energy Ea and kinetic factor  $k^\circ$ .

Fig. 7. Relationship between activation energy Ea and olivine content. The high-grade olivine is the sample used for derivation of the kinetic formula (F. Wang et al., 2019b) and thus the corresponding olivine content is considered as 100% for this kinetic formula.



**Fig. 8.** Relationship of predicted and practical data for Turnagain samples SN255–256, 258–262 under various temperatures.

$$\alpha = \left( 1 - \left( 1 - [S]^{0.7} \times [P_{CO_2}]^{1.6} \times [NaHCO_3]^{0.8} \times e^{\left( \frac{E_a - A}{B} - \frac{E_a \times 1000}{RT} \right) \times t} \right)^3 \right) \times f \quad (8)$$

The olivine content,  $f$ , can be determined by QXRD analysis. Once the activation energy is determined, the kinetic factor can be calculated for the kinetic formula to predict mineral carbonation efficiency and process conditions required. Through Equation (8), the comparison between the experimental and predicted data for each Turnagain sample SN254–SN256 and SN258–262 from the optimized kinetic formula is shown in Fig. 8. Herein, all experimental data had perfect matches with predicted data from the optimized kinetic formula under various temperatures, including dunite SN254. The maximum difference decreased to within  $\pm 4\%$ . This kinetic formula is completely quantitative on all important factors, not semi-empirical anymore.

Thus far, it has been verified that the quantitative kinetic model is robustly applicable to the mineral carbonation of natural silicate samples with an accuracy of  $\pm 4\%$  (absolute) when the carbonation process is controlled by the dissolution of olivine. The applicability of this

kinetic formula is not affected by the mineral composition, mineral carbonation capacity, specific surface area or the particle size distribution. The kinetic factor is dependant only on activation energy and olivine content. The final kinetic formula has been optimized for robust prediction of potential mineral carbonation behaviour.

In addition, in a combined process of mineral processing and mineral carbonation, the extent of carbonation of the minerals may be incomplete. In order to show the potential carbon sequestration ability and the potential for earning carbon credits for improving economics, it may be more interesting for the public and engineering to directly predict the sequestered  $CO_2$  amount based on Equation (5). For example, the carbonation capability for all the natural silicate samples can be calculated under the mineral carbonation conditions of  $175^\circ C$ ,  $PCO_2 = 34.5$  bar,  $1.5$  m  $NaHCO_3$  and  $10\%$  solids content, as shown in Fig. 9. The capabilities of a particular integrated process (mineral processing and mineral carbonation) may need to be re-calculated according to the detailed conditions. Nevertheless, this indicates that the kinetic formula is robust to estimate the potential of the carbon sequestration for an application.

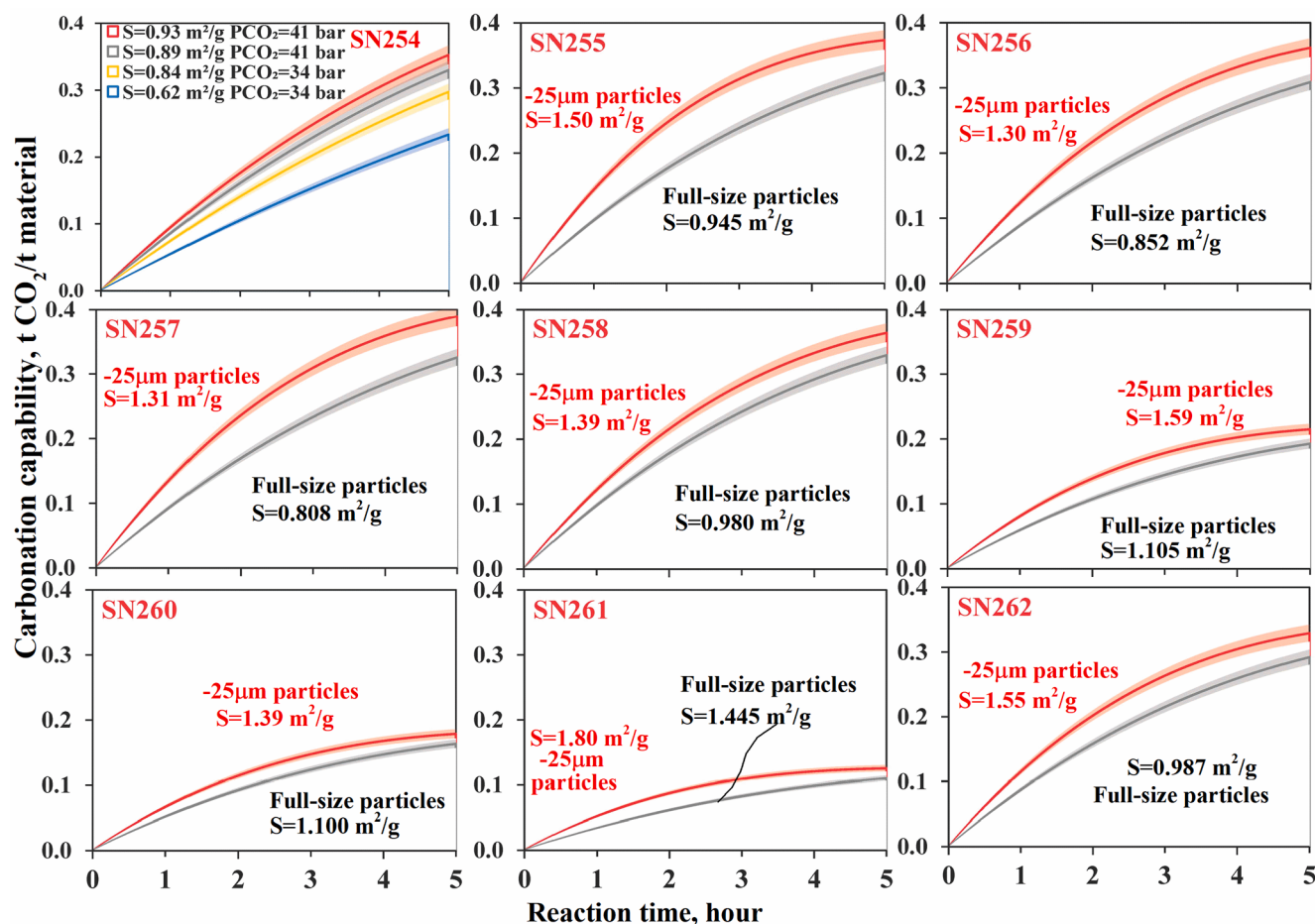


**Fig. 9.** Application of the kinetic formula to predicting carbonation capability (t CO<sub>2</sub>/t material) of various natural silicate samples under the conditions of 175 °C, PCO<sub>2</sub> = 34.5 bar, 1.5 m NaHCO<sub>3</sub> and 10% solids content.

#### 4. Conclusions

The quantified kinetic formula has been optimized into  $\alpha$

$$= \left( 1 - \left( 1 - [S]^{0.7} \times [P_{CO_2}]^{1.6} \times [NaHCO_3]^{0.8} \right. \right. \\ \left. \left. \times e^{\left( \frac{E_a - A}{B} - \frac{E_a \cdot 1000}{R T} \right) \times t} \right)^3 \right) \times f.$$

It can be robustly applied to mineral carbonation of various natural silicate samples when the carbonation rate was under chemical reaction control, regardless of mineral compositions, olivine content, mineral carbonation capacity, specific surface area and particle size distribution. The prediction precision of the kinetic formula was at most ±4% (absolute). The kinetic factor  $k^\circ$  is exponentially determined only by activation energy of carbonation of natural silicate samples. The suitable ranges of PCO<sub>2</sub>, temperature and addition of NaHCO<sub>3</sub> for application of this formula are 28 bar – 41 bar, 100 °C – 175 °C and 0.5 m – 1.5 m, respectively.

#### CRediT authorship contribution statement

**Fei Wang:** Project administration, Methodology, Investigation, Writing - original draft. **David Dreisinger:** Project administration, Supervision, Conceptualization, Writing - review & editing. **Mark Jarvis:**

Conceptualization, Resources. **Lyle Trytten:** Resources, Writing - review & editing. **Tony Hitchins:** Resources, Writing - review & editing.

#### Declaration of Competing Interest

The authors declare that they have no known competing financial interests or personal relationships that could have appeared to influence the work reported in this paper.

#### Acknowledgements

The authors thank the Natural Sciences and Engineering Research Council of Canada (NSERC) for the financial support of the collaborative research and development grants – projects (CRDPJ 523097 – 17). F. W. thanks the Killam Doctoral Scholarship and the Four-Year (4-YF) Fellowship of the University of British Columbia, and thanks Dr. Berend Wassink and Professor Edouard Asselin for technical support.

#### References

- Béarat, H., McKelvy, M.J., Chizmeshya, A.V.G., Gormley, D., Nunez, R., Carpenter, R.W., Squires, K., Wolf, G.H., 2006. Carbon sequestration via aqueous olivine mineral carbonation: Role of passivating layer formation. Environ. Sci. Technol. 40, 4802–4808. <https://doi.org/10.1021/es0523340>.
- Bourgeois, F., 2019. Chapter 9: CO<sub>2</sub> use. (2019) In: Meeting the dual challenge a roadmap to at-scale deployment of carbon capture, use, and storage. National Petroleum Council, Washington.
- Daval, D., 2018. Carbon dioxide sequestration through silicate degradation and carbon mineralisation: promises and uncertainties. npj Mater. Degrad. 2, 11. doi:10.1038/s41529-018-0035-4.

- Falini, G., Foresti, E., Gazzano, M., Gualtieri, A.E., Leoni, M., Lesci, I.G., Roveri, N., 2004. Tubular-shaped stoichiometric chrysotile nanocrystals. *Chem. - A Eur. J.* 10, 3043–3049. <https://doi.org/10.1002/chem.200305685>.
- Gadikota, G., Matter, J., Kelemen, P., Park, A.-H.A., 2014. Chemical and morphological changes during olivine carbonation for CO<sub>2</sub> storage in the presence of NaCl and NaHCO<sub>3</sub>. *Phys. Chem. Chem. Phys.* 16, 4679–4693. <https://doi.org/10.1039/c3cp54903h>.
- Hamilton, J.L., Wilson, S.A., Morgan, B., Harrison, A.L., Turvey, C.C., Paterson, D.J., Dipple, G.M., Southam, G., 2020. Accelerating mineral carbonation in ultramafic mine tailings via direct CO<sub>2</sub> reaction and heap leaching with potential for base metal enrichment and recovery. *Econ. Geol.* 115, 303–323. <https://doi.org/10.5382/econgeo.4710>.
- Hasan, S.N.M.S., Kusin, F.M., 2018. Potential of mining waste from metallic mineral industry for carbon sequestration. *IOP Conference Series: Materials Science and Engineering*, 458 (1), 12013. <https://doi.org/10.1088/1757-899X/458/1/012013>.
- Hitch, M., Dipple, G.M., 2012. Economic feasibility and sensitivity analysis of integrating industrial-scale mineral carbonation into mining operations. *Miner. Eng.* 39, 268–275. <https://doi.org/10.1016/j.mineng.2012.07.007>.
- International Energy Agency, I., 2016. Technology roadmap - Low-carbon transition in the cement industry, World Business Council For Sustainable Development (WBCSD). doi:10.1007/springerreference\_7300.
- Lackner, K.S., 2003. A guide to CO<sub>2</sub> sequestration. *Science* 300, 1677–1678. <https://doi.org/10.1126/science.1083529>.
- Li, J., Hitch, M., 2016. Mechanical activation of ultramafic mine waste rock in dry condition for enhanced mineral carbonation. *Miner. Eng.* 95, 1–4. <https://doi.org/10.1016/j.mineng.2016.05.020>.
- Li, Q., Gupta, S., Tang, L., Quinn, S., Atakan, V., Riman, R.E., 2016. A novel strategy for carbon capture and sequestration by rHLPD processing. *Front. Energy Res.* 3, 53. <https://doi.org/10.3389/fenrg.2015.00053>.
- Matter, J.M., Kelemen, P.B., 2009. Permanent storage of carbon dioxide in geological reservoirs by mineral carbonation. *Nat. Geosci.* 2, 837–841. <https://doi.org/10.1038/ngeo683>.
- Matter, J.M., Stute, M., Snaebjörnsdóttir, S., Oelkers, E., Gislason, S.R., Aradottir, E.S., Sigfusson, B., Gunnarsson, I., Alfredsson, H.A., Wolff-boenisch, D., Mesfin, K., Dideriksen, K., Broecker, W.S., 2016. Rapid carbon mineralization for permanent disposal of anthropogenic carbon dioxide emissions. *Science* 352, 1312–1314.
- Mbrtrnr, M., 1982. The crystal structure of lizardite 1T: hydrogen bonds and polytypism. *American Mineralogist*, 67, 587–598.
- O'Connor, W.K., Dahlin, D.C., Nilsen, D.N., Walters, R.P., 2001. Carbon dioxide sequestration by direct aqueous mineral carbonation. [osti.gov 11](https://www.osti.gov/11).
- O'Connor, W.K., Dahlin, D.C., Rush, G.E., Gerdemann, S.J., Penner, L.R., Nilsen, D.N., 2005. Aqueous mineral carbonation: Mineral availability, pretreatment, reaction parametrics and process studies.
- Oelkers, E.H., Declercq, J., Saldi, G.D., Gislason, S.R., Schott, J., 2018. Olivine dissolution rates: A critical review. *Chem. Geol.* 500, 1–19. <https://doi.org/10.1016/j.chemgeo.2018.10.008>.
- Olajire, A.A., 2013. A review of mineral carbonation technology in sequestration of CO<sub>2</sub>. *J. Pet. Sci. Eng.* 109, 364–392. <https://doi.org/10.1016/j.petrol.2013.03.013>.
- Pan, S.-Y., Chen, Y.-H.H., Fan, L.-S., Kim, H., Gao, X., Ling, T.-C., Chiang, P.-C.C., Pei, S.-L., Gu, G., 2020. CO<sub>2</sub> mineralization and utilization by alkaline solid wastes for potential carbon reduction. *Nat. Sustain.* 4, 41. <https://doi.org/10.1038/s41893-020-0486-9>.
- Power, I.M., Wilson, S.A., Dipple, G.M., 2013. Serpentinite carbonation for CO<sub>2</sub> sequestration. *Elements* 9, 115–121. <https://doi.org/10.2113/gselements.9.2.115>.
- Renforth, P., Washbourne, C.L., Taylder, J., Manning, D.A.C., 2011. Silicate production and availability for mineral carbonation. *Environ. Sci. Technol.* 45, 2035–2041. <https://doi.org/10.1021/es103241w>.
- Sanna, A., Uibu, M., Caramanna, G., Kuusik, R., Maroto-Valer, M.M., 2014. A review of mineral carbonation technologies to sequester CO<sub>2</sub>. *Chem. Soc. Rev.* 43, 8049–8080. <https://doi.org/10.1039/C4CS00035H>.
- Scarlett, N.V.Y., Madsen, I.C., 2006. Quantification of phases with partial or no known crystal structures. *Powder Diffr.* 21, 278–284. <https://doi.org/10.1154/1.2362855>.
- Seifritz, W., 1990. CO<sub>2</sub> disposal by means of silicates. *Nature*. <https://doi.org/10.1038/345486b0>.
- Stopic, S., Dertmann, C., Koiwa, I., Kremer, D., Wotruba, H., Etzold, S., Telle, R., Knops, P., Friedrich, B., 2019. Synthesis of nanosilica via olivine mineral carbonation under high pressure in an autoclave. *Metals (Basel)*. 9, 708. <https://doi.org/10.3390/met9060708>.
- Tomkinson, T., Lee, M.R., Mark, D.F., Smith, C.L., 2013. Sequestration of Martian CO<sub>2</sub> by mineral carbonation. *Nat. Commun.* 4, 2662. <https://doi.org/10.1038/ncomms3662>.
- Wang, F., Dreisinger, D., Jarvis, M., Hitchins, T., 2021. Kinetic evaluation of mineral carbonation of natural silicate samples. *Chem. Eng. J.* 404, 126522 <https://doi.org/10.1016/j.cej.2020.126522>.
- Wang, F., Dreisinger, D., Jarvis, M., Hitchins, T., 2019a. Kinetics and mechanism of mineral carbonation of olivine for CO<sub>2</sub> sequestration. *Miner. Eng.* 131, 185–197. <https://doi.org/10.1016/j.mineng.2018.11.024>.
- Wang, F., Dreisinger, D., Jarvis, M., Hitchins, T., Dyson, D., 2019b. Quantifying kinetics of mineralization of carbon dioxide by olivine under moderate conditions. *Chem. Eng. J.* 360, 452–463. <https://doi.org/10.1016/j.cej.2018.11.200>.
- Wang, F., Dreisinger, D.B., Jarvis, M., Hitchins, T., 2018. The technology of CO<sub>2</sub> sequestration by mineral carbonation: current status and future prospects. *Can. Metall. Q.* 57, 46–58. <https://doi.org/10.1080/00084433.2017.1375221>.
- Wang, J., Watanabe, N., Okamoto, A., Nakamura, K., Komai, T., 2019c. Pyroxene control of H<sub>2</sub> production and carbon storage during water-peridotite-CO<sub>2</sub> hydrothermal reactions. *Int. J. Hydrogen Energy*. 44, 26835–26847. <https://doi.org/10.1016/j.ijhydene.2019.08.161>.
- Wood, C.E., Qafoku, O., Loring, J.S., Chaka, A.M., 2019. Role of Fe(II) content in olivine carbonation in wet supercritical CO<sub>2</sub>. *Environ. Sci. Technol. Lett.* 6, 592–599. <https://doi.org/10.1021/acs.estlett.9b00496>.
- Xi, F., Davis, S.J., Ciais, P., Crawford-Brown, D., Guan, D., Pade, C., Shi, T., Syddall, M., Lv, J., Ji, L., Bing, L., Wang, J., Wei, W., Yang, K.H., Lagerblad, B., Galan, I., Andrade, C., Zhang, Y., Liu, Z., 2016. Substantial global carbon uptake by cement carbonation. *Nat. Geosci.* 9, 880–883. <https://doi.org/10.1038/ngeo2840>.